ASEG-PESA 2015
Geophysics and Geology together for Discovery
24th International Geophysical Conference and Exhibition
15–18 February 2015 Perth, Western Australia

Constraining gravity gradient inversion with a source depth volume

Cericia Martinez[1] **Daniel Wedge**[2] **Yaoguo Li**[1] **Eun-Jung Holden**[2]
[1]*Center for Gravity, Electrical, and Magnetic Studies, Department of Geophysics, Colorado School of Mines*
[2]*Centre for Exploration Targeting, The University of Western Australia*

SUMMARY

Efficiently extracting the maximum amount of information from gravity gradient data is challenging. Interpretation often takes place in either the data domain or model domain. Here, we present a workflow that utilizes two interpretation techniques that can result in better characterization of the subsurface. Using a method that estimates depth to source, we obtain a depth volume of estimated source locations. The depth volume is then used to constrain inversion of gravity gradient data in the form of a reference model and 3D model weighting. We demonstrate that this combined approach improves the ability to recover sources at depth.

Key words: gravity inversion, constrained density model

INTRODUCTION

Inversion of gravity gradient data has become a commonly accepted method to simultaneously interpret multiple components, resulting in a density model of the subsurface. Given the lack of depth information in potential field data, algorithms have employed various strategies to overcome these inherent difficulties. One such approach is to constrain the inversion through incorporation of prior geologic information (Guillen et al., 2008; Lelièvre et al., 2009; Ailleres et al., 2010). A reference model provides a versatile way to incorporate known structure, source depths, and known physical properties into inversion. A second avenue for incorporation of prior information is through a weighting function. The weighting function provides a mechanism to incorporate uncertainty in the reference model or other subsurface constraints (Oldenburg and Li, 2005).

While a reference model or weighting function can be created from borehole or other geologic information, we instead focus on the use of the gravity gradient data itself. From the gradient data, depth to anomalous source estimates can be obtained. In the context of the magnetic method, estimating the depth to source has been widely explored. Much of the work has likewise been extended to the gravity method, and more recently gravity gradiometry. In particular, Zhang et al. (2000) and Mikhailov et al. (2007) illustrate variations of Euler deconvolution to estimate source locations from gravity gradient data. Beiki and Pedersen (2010) perform an eigenvalue decomposition and use a least squares method to estimate the source location, assuming point mass sources. Building upon the approach by Beiki and Pedersen, we similarly utilize an eigenvector-based method to generate an accumulation volume representing the depths to anomalous masses (Wedge, 2013). Using such an accumulation scheme, the assumption of point mass sources is no longer necessary and linear or otherwise shaped features can be identified.

From the accumulation volume, a reference model or weighting function can be constructed and used as a constraint in the inversion of the gravity gradient data. We demonstrate the advantages of incorporating additional information on source depths derived from gravity gradient data.

SOURCE DEPTH ESTIMATES

An accumulation volume representing probable depths of anomalous masses is generated using an eigenvalue decomposition of the gravity gradient tensor (Wedge, 2013). The tensor is diagonalized yielding three eigenvectors and three eigenvalues. The eigenvector ($\overrightarrow{v_1}$) used to create the accumulation volume is that corresponding to the largest eigenvalue (λ_1). As Pedersen and Rasmussen (1990) show, the eigenvector ($\overrightarrow{v_1}$) has the unique property of pointing towards the anomalous centre of mass. This property is exploited in order to create a representative depth volume.

First, the subsurface area is discretized into rectangular prisms. The data are band pass filtered at pre-defined frequencies. Each frequency band are then used to generate an accumulation volume as follows. For each data location, the eigenvector, $\overrightarrow{v_1}$, is calculated and projected from the observation point through the extent of the discretized volume. The value of each prismatic cell that the projected vector passes through is increased by one. The eigenvector projection is carried out for all observation locations, resulting in an accumulated volume representing the number of times a $\overrightarrow{v_1}$ eigenvector pointed towards each prism for that particularly frequency band of the data.

The accumulation volumes from each frequency band are then summed resulting in a volume where higher cell values represent probable locations of mass anomalies. Separating the data into frequency bands reduces the effect of noise since the higher frequency bands can be left out of the final accumulation volume. During the accumulation process, a radius of influence is defined so that all prisms within the radius of $\overrightarrow{v_1}$ likewise have their accumulation values increased by one. This also helps to mitigate the effect of noise by accounting for error in the eigenvector direction.

Before moving onto inversion, we make a few remarks about estimating the depth to source method summarized above. Estimating source depths based on frequency bands, gives equal weight to both shallow and deep sources. Given the sensitivity of gravity gradient data to shallow sources, the ability to identify sources at depth can be advantageous. Increasing the accumulation value by one likewise ensures both shallow and deep masses are represented.

INVERSION

We use the 3D potential-field inversion algorithm developed by Li (2001a) and Li and Oldenburg (2003) to invert the gravity gradient data. For the construction here, we specify a right hand Cartesian system where *x* is northing, *y* is easting, and *z* points vertically down. The algorithm assumes a set of contiguous rectangular prisms each with a constant density contrast. The inverse solution is obtained using Tikhonov regularization by minimizing a total objective function,

$$\begin{array}{c} \min \\ \text{subject to} \end{array} \quad \begin{array}{c} \phi = \phi_d + \mu\phi_m \\ \vec{\rho}_{min} \leq \vec{\rho} \leq \vec{\rho}_{max} \end{array} \qquad (1)$$

where μ is a regularization parameter, ϕ_d and ϕ_m are data misfit and model objective functions, respectively. Lower, $\vec{\rho}_{min}$, and upper, $\vec{\rho}_{max}$, bound constraints can be imposed on the recovered density contrast. The reference model (ρ_0) and weighting functions (w_s,w_x,w_y,w_z) are present in the model objective function ϕ_m as shown in equation 2.

$$\begin{aligned} \phi_m(\rho) \quad = \quad & \int_V w_s[w(z)(\rho - \rho_0)]^2 dv \\ + \quad & L_x^2 \int_V w_x \left[\frac{\partial w(z)(\rho - \rho_0)}{\partial x}\right]^2 dv \\ + \quad & L_y^2 \int_V w_y \left[\frac{\partial w(z)(\rho - \rho_0)}{\partial y}\right]^2 dv \\ + \quad & L_z^2 \int_V w_z \left[\frac{\partial w(z)(\rho - \rho_0)}{\partial z}\right]^2 dv \end{aligned} \qquad (2)$$

Inclusion of a reference model (ρ_0) penalizes the recovered model as it deviates from the reference model. In regions of high uncertainty the weighting functions (w_s,w_x,w_y,w_z) can be assigned low weights so as to not penalize the model if it deviates from the reference model. Low weighting values for the derivative weighting functions w_x, w_y, and w_z allow for the presence of high gradients in those regions.

The accumulation volume described in the preceding section can be considered a representative likelihood volume for source depth location. Two ways of incorporating the information encapsulated within the accumulation volume into inversion are through the reference or weighting functions. Next, we illustrate the advantages of incorporating the accumulation into inversion.

SYNTHETIC EXAMPLE WORKFLOW

We illustrate the workflow through a synthetic dataset. Six components of the gravity gradient tensor are contaminated with 2 Eo Gaussian noise and shown in Figure 1. The anomalies represent the sources listed in Table 1. The subsurface is discretized into 10 m cubes in order to generate the accumulation volume. The radius of influence is set to 100 m. The accumulation volume is then converted to a coarser cell size of 50 m cubes for use in inversion.

Prior to inverting, we denoise the data using an equivalent source technique (Li, 2001b). Due to space constraints, only the denoised T_{zz} component is shown in Figure 2, with labelled source anomalies corresponding to Table 1.

Label	Shape	$\Delta\rho$ (g/cc)	Depth (m)
A	Block	+0.20	500 – 900
B	Sheet	+0.15	0 – 1000
C	Sphere	+0.30	50 – 350
D	Cone	-0.40	150 – 350
E	Tunnel	-2.70	3 – 7

Table 1: Index of source bodies generating data shown in Figure 1 and labelled in Figure 2.

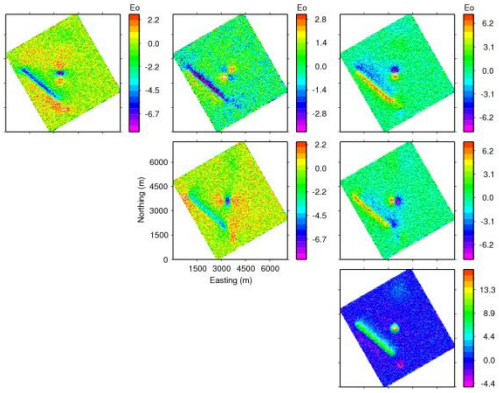

Figure 1: Synthetic gravity gradient data resulting from five geometric sources described in Table 1. Simulated altitude is at 400 m.

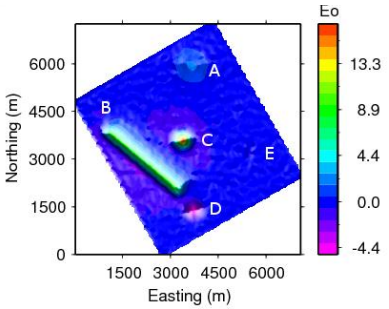

Figure 2: Denoised T_{zz} with anomaly sources labelled according to Table 1.

The data are first inverted without inclusion of a reference model. The density contrast within the recovered model is allowed to vary between -5 g/cc and 5 g/cc in all cases. Depth slices through the recovered model are shown in the first row of Figure 4. In what follows, we call this unconstrained model the base model for comparison purposes.

Reference model from accumulation volume

In order to incorporate the depth estimates obtained from the method described above, the accumulation model must be converted into a representative density model. The constructed density model can then be used as a reference model in inversion. We first implement various accumulation-density conversions then invert the gravity gradient data with the constructed reference models.

Three reference models are generated by normalizing the accumulation values to three different density ranges. The three ranges are selected so the reference model density contrasts are either too small, too large, or entirely positive. The accumulation values range from 0 to 20412. The accumulation volume is normalized to lie in the density range (-0.095,0.186) g/cc for Reference Model A, which is too small. The density range for Reference Model B is (0,1) and

Reference Model C is (-0.095,1). The accumulation value range for Reference model C uses only non-zero values for normalization; the minimum accumulation value is positive.

A depth slice at 300 m through each reference model is shown in Figure 3 plotted on a colorscale of (-0.1,0.4) g/cc. Here, the most clearly defined feature lies in the centre of the models (corresponding to the sphere). The calculated T_{zz} response for each reference model is also given in Figure 3. Comparing the response calculated from the reference models to the denoised T_{zz} in Figure 2, it is evident that the reference model is an inaccurate representation of the actual density distribution.

Slices through the recovered models from inverting the data using each reference model are shown in Figure 4. Using Reference Model A (row 2), the block, sheet, and sphere are identified with positive density contrast. The continuity of the sheet feature begins to fade just after 600 m, with the edges being recovered until a depth of roughly 800 m. The positive density range imposed by Reference Model B (row 3) imposes too much structure around the source bodies. Reference Model C (row 4) smears the sphere and block source well beyond the known extent.

In the unconstrained recovered model, the buried sphere and depth extent of the sheet are not well resolved. Using the accumulation volume as a reference, helps the inversion to resolve the buried sphere and constrains the width of the sheet at depth. The negative density feature to the south of the sheet is present in the recovered models in the near surface, but is not necessarily distinguishable from the average recovered background values. The embedded tunnel feature is much smaller than a single cell, and is not expected to be resolved.

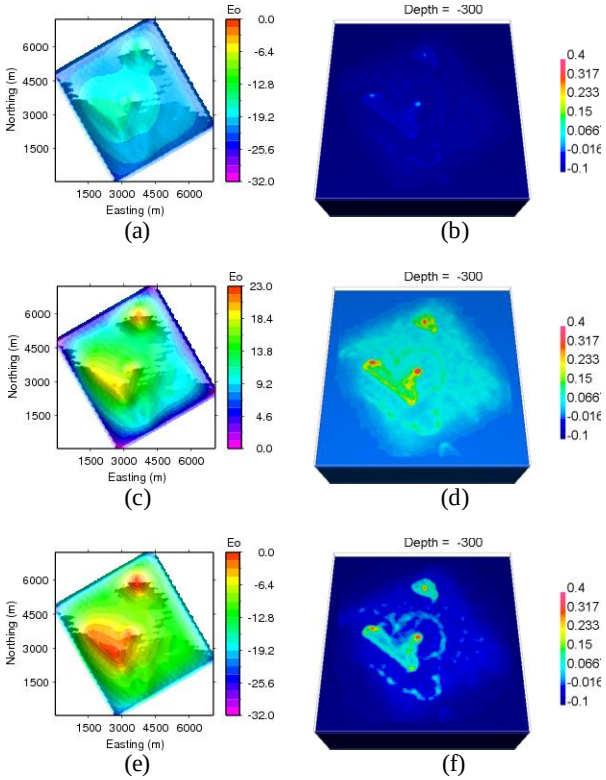

Figure 3: Forward modelled T_{zz} and depth slice at 300 m for: (a)-(b) Reference Model A; (c)-(d) Reference Model B; (e)-(f) Reference Model C. In the three reference model images, the colourbar ranges from -0.1 to 0.4, where cells larger than 0.4 are red and cells lower than -0.1 are blue.

Weighting function from accumulation volume

Next we utilize the accumulation volume as a 3D weighting function. In the model objective function of equation 2, four weights (w_s,w_x,w_y,w_z) can be adjusted. The accumulation volume is first normalized to range from 0 to 100. The 3D weighting function is obtained by taking one divided by the normalized accumulation values and assigned to the smallest model 3D weighting function, w_s. For simplicity, the weighting functions and length scales (L_x,L_y,L_z) for the gradient terms are set to be small so that the smallest model term dominates. Slices through the recovered model using the 3D weighting function are shown in row five of Figure 4. The last row of Figure 4 shows the recovered model using both the 3D weighting function and reference model A.

Using just a weighting function further distinguishes that there is a source at depth in the northern region of the model. The model in general has higher values than the base model. The width of the sheet feature is tightened at 600 m depth and the buried block is better recovered as compared to the base model. Using a reference model along with the model weighting results in structure at depth. The combined constraints do not necessarily improve upon the two separately recovered models using only a reference (Figure 4, row 2) or only 3D weights (Figure 4, row 5).

CONCLUSIONS

The three reference models illustrate that regardless of the density range (too large, too small, positive only) utilizing the accumulation volume assists in resolving source bodies at depth. The recovered density contrast values are affected by the reference model, and the conversion of accumulation to density should ideally utilize known densities in order to appropriately scale the volume. Incorporating the accumulation volume depth information in the form of 3D weights overcomes the need to convert to a density model. As a 3D weighting function, the accumulation volume significantly increases the ability to recover sources at depth.

ACKNOWLEDGMENTS

This work was supported in part by the industry consortium "Gravity and Magnetics Research Consortium" (GMRC) at the Colorado School of Mines. The current sponsoring companies are Anadarko, Bell Geospace, BG Group, BGP International, BP, CGG, ConocoPhillips, ExxonMobil, Gedex, Lockheed Martin, Marathon Oil, Micro-g LaCoste, Petra Energia, Petrobras, Shell, Tullow Oil, and Vale.

REFERENCES

Ailleres, L., M. Lindsay, M. Jessell, and E. DeKemp, 2010, The role of geological uncertainty in developing combined geological and potential field inversions: ASEG Extended Abstracts 2010, 1–4.

Beiki, M., and L. B. Pedersen, 2010, Eigenvector analysis of gravity gradient tensor to locate geologic bodies: Geophysics, 75, I37–I49.

Guillen, A., P. Calcagno, G. Courrioux, A. Joly, and P. Ledru, 2008, Geological modelling from field data and geological knowledge Part II. Modelling validation using gravity and magnetic data inversion: Physics of the Earth and Planetary Interiors, 171, 158–169.

Lelièvre, P. G., D.W. Oldenburg, and N. C.Williams, 2009, Integrating geological and geophysical data through advanced constrained inversions: Exploration Geophysics, 40, 334–341.

Li, Y., 2001a, 3-d inversion of gravity gradiometer data: SEG Technical Program Expanded Abstract, 20, 1470–1473.

———, 2001b, Processing gravity gradiometer data using an equivalent source technique: 1466–1469.

Li, Y., and D.W. Oldenburg, 2003, Fast inversion of large-scale magnetic data using wavelet transforms and logarithmic barrier method: Geophysical Journal International, 152, 251–265.

Mikhailov, V., G. Pajot, M. Diament, and A. Price, 2007, Tensor deconvolution: A method to locate equivalent sources from full tensor gravity data: Geophysics, 72, I61–I69.

Oldenburg, D., and Y. Li, 2005, 5, in 5. Inversion for Applied Geophysics: A Tutorial: 89–150.

Pedersen, L. B., and T. M. Rasmussen, 1990, The gradient tensor of potential field anomalies: Some implications on data collection and data processing of maps: Geophysics, 55, 1558–1566.

Wedge, D., 2013, Mass anomaly depth estimation from full tensor gradient gravity data: Applications of Computer Vision (WACV), 2013 IEEE Workshop on, 526–533.

Zhang, C., M. F. Mushayandebvu, A. B. Reid, J. D. Fairhead, and M. E. Odegard, 2000, Euler deconvolution of gravity tensor gradient data: Geophysics, 65, 512.

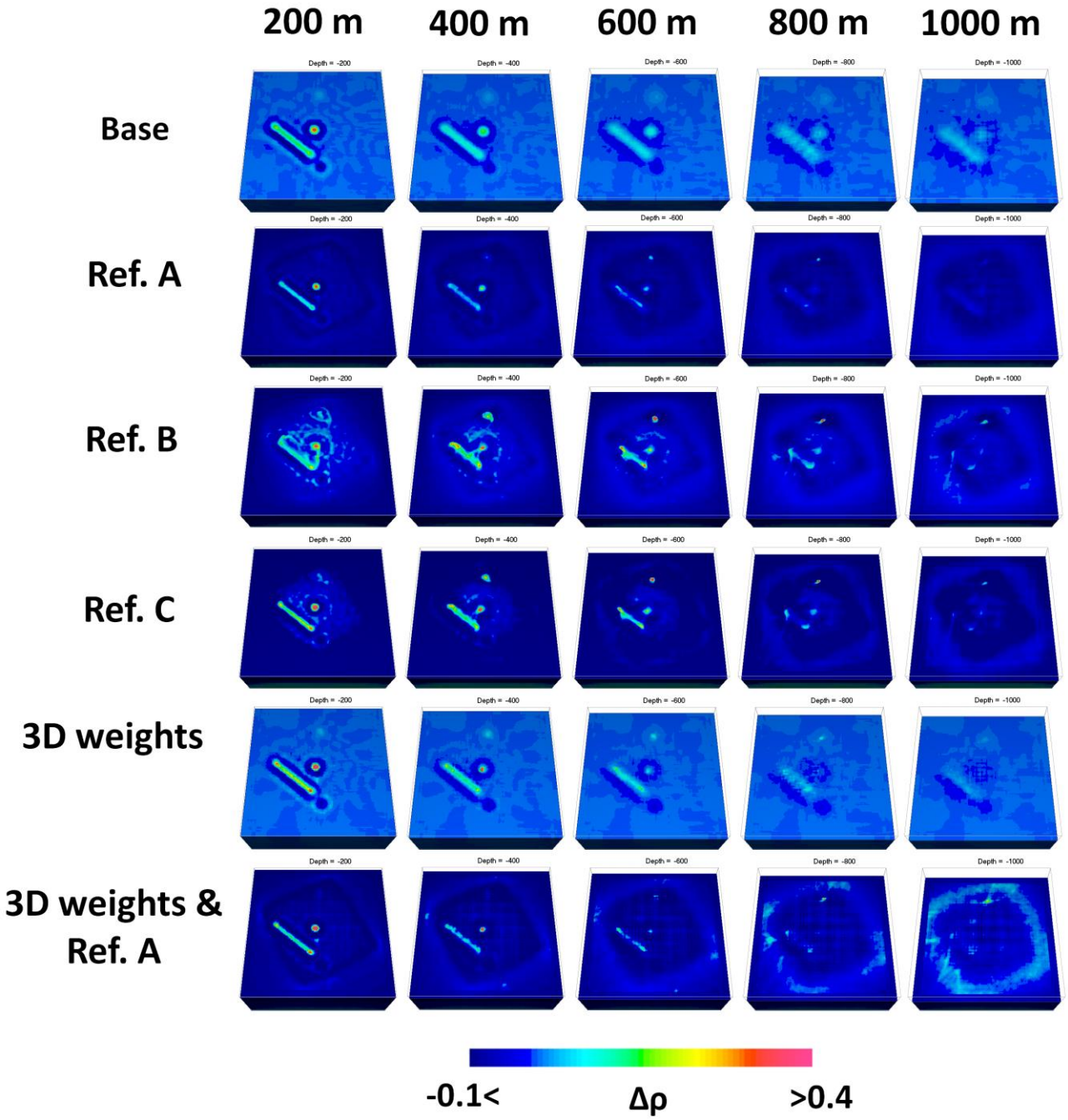

Figure 4: Recovered model depth slices for: unconstrained inversion (row 1), inversion with reference model A (row 2), inversion with reference model B (row 3), inversion with reference model C (row 4), inversion with 3D weights (row 5), inversion with 3D weights and reference model A (row 6). All models are visualized with the same colourscale, where cells less than -0.1 are blue and cells greater than 0.4 are red.